

Graphite on graphite

G.E. Volovik^{1,2,3} and V.M. Pudalov^{3,4}

¹*Low Temperature Laboratory, Aalto University, P.O. Box 15100, FI-00076 Aalto, Finland*

²*Landau Institute for Theoretical Physics RAS, Kosygina 2, 119334 Moscow, Russia*

³*P. N. Lebedev Physical Institute of the RAS, Moscow 119991, Russia*

⁴*National Research University Higher School of Economics, Moscow 101000, Russia*

(Dated: March 1, 2022)

We propose potential geometry for fabrication of the graphite sheets with atomically smooth edges. For such sheets with Bernal stacking, the electron-electron interaction and topology should cause sufficiently high density of states resulting in the high temperature of either spin ordering or superconducting pairing.¹

PACS numbers:

The perspective direction in increasing the critical temperature of superconductivity is the search for and synthesis of the electronic systems with flat band in the energy spectrum. The dispersionless energy spectrum has a singular density of states, which provides the transition temperature being proportional to the coupling constant instead of the exponential suppression.² There are different potential sources of flat band.

One of them is formation of the so-called Khodel-Shaginyan fermion condensate – the flat band caused by electron-electron interaction in metals²⁻⁴. This is the manifestation of the general phenomenon of the energy level merging due to electron-electron interaction. This effect has been recently suggested⁵ to be responsible for merging of the discrete energy levels in two-dimensional electron system in quantizing magnetic fields. Another case of merging was found on the verge of the metal-insulator transition or quantized Hall effect to insulator transition, where energy levels for difference subbands merge instead of repulse⁶⁻⁸.

According to Ref.⁹ the favourable condition for the formation of such flat band is when the van Hove singularity comes close to the Fermi surface² (see also Ref.¹⁰ for the simple Landau type model of the formation of such flat band). It is also possible that this effect is responsible for the occurrence of superconductivity with high T observed in the pressurized sulfur hydride^{11,12}. There are some theoretical evidences^{13,14} that the high- T_c superconductivity takes place at such pressure, when the system is near the Lifshitz transition, i.e. when the Fermi surface is close to van Hove singularity and the bands flatten. That is why it is not excluded that the Khodel-Shaginyan flat band is formed in sulfur hydride at pressure 180-200 GPa giving rise to high- T_c superconductivity.

The flat band can be also formed in such semimetals which contain the Dirac lines. Dirac nodal lines are the topologically protected lines in the energy spectrum, which have zero energy¹⁵⁻¹⁹. The flat band appears on the surface of such material due to the topological phenomenon of the bulk-edge correspondence. The boundary of the surface flat band is determined by the projection of the Dirac line in the bulk to the plane of the surface. By now, there are many evidences of the existence of Dirac lines in the electronic spectrum of semimetals²⁰⁻²⁸.

The Dirac nodal lines and the corresponding flat bands exist also in the pair-correlated systems: in cuprate superconductors and in the spectrum of fermionic excitations in the recently discovered polar phase of superfluid ^3He ²⁹. They lead to the singularity in the density of states of the fermions bound to the vortex.³⁰⁻³²

Graphite is one of the realizations of the approximate nodal line semimetal (for the review, see¹⁹). In the model, where some small hopping elements are neglected, the Bernal graphite has two vertical Dirac lines running between the \mathbf{H} points in the 3D graphite band structure. According to the bulk-edge correspondence, the Dirac line in bulk along the normal to the graphite planes produces the zero energy states on the lateral boundaries of Bernal graphite, which form the surface flat band. This 2D flat band can be considered as extension of the 1D flat band states in graphene with zigzag edges¹⁹. Note that in the similar model of the rhombohedral graphite the Dirac line forms a spiral, whose projection on the horizontal boundary marks the boundary of the flat band. In the Bernal graphite model the flat band exists only on the lateral boundary.

In the real graphite the flat band is distorted due to two reasons. The first is due to the higher-order hopping elements, which are neglected in the model. These elements break the symmetry, which supports the topological stability of the Dirac line. In real Bernal and rhombohedral graphite the Dirac line transforms to the electron and hole pockets³³. The topology of the Dirac lines, however, is not fully destroyed: the electron and hole pockets form the continuous chain. Nevertheless, the extension of the Dirac line to the chain of Fermi surfaces distorts the surface flat band. Whether such distortion of the flat band considerably reduces the high transition temperature expected for the flat band materials is to be investigated both numerically and experimentally. The flattening of the spectrum for the five layers of graphene with the rhombohedral ABCAB stacking has been observed experimentally³⁴ by epitaxial growing on 3C-SiC(111) on 2offaxis 6H-SiC(0001). Note that there can be the combined effect of topology and

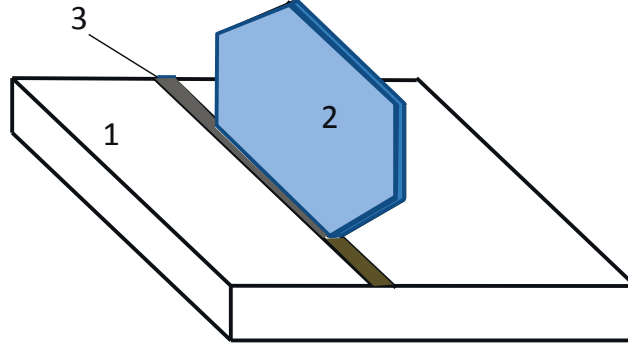


FIG. 1: Schematic view of the graphite-on-graphite design. 1 – graphite (BN) substrate, 2 - graphite (or a multilayered graphene) sheet, or a graphite wall, 3 – a strip of the catalyst.

electron-electron interaction for the stabilization of the flat band, i.e. due to the interaction a part of the approximate flat band may become exact.

However, there is another important source of distortion of the edge flat band in Bernal graphite: the lateral walls of graphite are always rough. This is not important for the rhombohedral graphite, where the (approximate) Dirac lines are not vertical and thus have nonzero projection on the smooth horizontal boundary. That is why we need such configuration of the Bernal graphite, where the lateral walls can be made smooth.

In order to fabricate smooth lateral walls, one obvious way is to cut the graphite edge with a nanometer precision by using scanning tunneling lithography^{35,36}; in this way graphene nanoribbons with smooth edges were obtained in Ref.³⁷. The graphite flakes may be shaped using Ar- or He-ion beam etching.

Without relying on lithographic techniques, fabrication of nanoribbons with atomically smooth edges has also been reported via the so-called “bottom-up” processes – epitaxial growth on templated nanofacets³⁸ and by chemical vapor deposition on surface features^{39–41}. Recently, graphene nanoribbons with atomically flat edges have been grown on a semiconductor Ge-wafer⁴².

Another way to grow graphene/graphite sheets orthogonal to the atomically flat graphite substrate is shown schematically in Fig. 1. In order to facilitate such growth, an atomically thin and narrow strip of a catalyst (Pt, Ni or TiC) may be deposited at the flat surface of a crystalline substrate (graphite, (001)Ge, h-BN, etc) in the proper direction. Alternatively, growth in the out-of-plane direction may be initiated by surface features such as trenches, steps or ridges. Then, in the CVD reactor the graphite sheets may start growing perpendicular to the substrate plane and directed along the strip.

The growth conditions in the proposed geometry, of course, require more thorough consideration. We note, however, that it is similar to the “carbon nanowalls” which are graphite nanostructures with edges comprised of stacked planar graphene sheets standing vertically on a substrate. The sheets form a wall structure with thicknesses in the range of a few nanometers to a few tens of nanometers⁴³.

In the case of success, the interface between the vertical graphite and the horizontal graphite layers may be made smooth. With the appropriate mutual orientations of the interface and crystal axes, the flat interface contains the (approximate) flat band, and may have sufficiently large density of states to produce the high temperature of transition to either magnetic or superconducting state. Graphene itself also may serve as substrate.

At the moment there are many evidences of enhanced superconducting transition temperature, which are related to monolayers⁴⁴, interfaces^{45–50}, alkanes in contact with a graphite surface⁵¹, polymer composites with embedded graphene flakes^{52,53}, etc. The interface itself may provide the factor which together with the electron-electron interaction enhances the effect of the flat band singularity in the electronic density of states leading to unexpected effects.

VP benefited from discussions with K. N. Eltsov and E. D. Obraztsova. The authors acknowledge support by RSCF (# 16-42-01100).

¹ This is the English translation of the Russian version published in: *Pis'ma ZhETF* **104**, 888–891 (2016).

- ² V.A. Khodel and V.R. Shaginyan, Superfluidity in system with fermion condensate, JETP Letters **51**, 553 (1990).
- ³ G.E. Volovik, A new class of normal Fermi liquids, JETP Lett. **53**, 222 (1991).
- ⁴ P. Nozieres, Properties of Fermi liquids with a finite range interaction, J. Phys. (Fr.) **2**, 443 (1992).
- ⁵ A.A. Shashkin, V.T. Dolgoplov, J.W. Clark, V.R. Shaginyan, M.V. Zverev and V.A. Khodel, Merging of Landau levels in a strongly-interacting two-dimensional electron system in silicon, Phys. Rev. Lett. **112**, 186402 (2014).
- ⁶ V.M. Pudalov, M.D'Iorio, J.Campbell, Hall resistane and Quantized Hall effect to insulator transitions in a 2D electron system, Pis'ma ZhETF **57**(9), 592 (1993); JETP Lett. **57**(9), 608 (1993).
- ⁷ S.V.Kravchenko, W.Mason, J.Furneaux, V.M.Pudalov, Global phase diagram for the Quantum Hall Effect: an experimental picture, Phys. Rev. Lett., **75**, 910 (1995).
- ⁸ V.M. Pudalov, M.D'Iorio, Termination of the quantum Hall effect by the electron solid, Surface Science, **305**, 107 (1994).
- ⁹ D. Yudin, D. Hirschmeier, H. Hafermann, O. Eriksson, A.I. Lichtenstein, M.I. Katsnelson, Fermi condensation near van Hove singularities within the Hubbard model on the triangular lattice, Phys. Rev. Lett. **112**, 070403 (2014).
- ¹⁰ G.E. Volovik, On Fermi condensate: near the saddle point and within the vortex core, JETP Lett. **59**, 830 (1994).
- ¹¹ A.P. Drozdov, M.I. Erements, and I.A. Troyan, Conventional superconductivity at 190 K at high pressures, IEEE/CSC & ESAS SUPERCONDUCTIVITY NEWS FORUM (global edition), January 2015, arXiv:1412.0460.
- ¹² A.P. Drozdov, M.I. Erements, I.A. Troyan, V. Ksenofontov, S.I. Shylin, Conventional superconductivity at 203 K at high pressures, Nature **525**, 73 (2015)
- ¹³ Yundi Quan and W.E. Pickett, Impact of van Hove singularities in the strongly coupled high temperature superconductor H₃S, Phys.Rev. B **93** 104526 (2016).
- ¹⁴ A. Bianconi and T. Jarlborg, Superconductivity above the lowest Earth temperature in pressurized sulfur hydride, EPL **112**, 37001 (2015); A. Bianconi and T. Jarlborg, Lifshitz transitions and zero point lattice fluctuations in sulfur hydride showing near room temperature superconductivity, Novel Superconducting Materials **1**, 15 (2015); T. Jarlborg and A. Bianconi, Breakdown of the Migdal approximation at Lifshitz transitions with a giant zero-point motion in H₃S superconductor, Sci. Rep. **6**, 24816 (2016); A. Bussmann-Holder, J. Kohler, M.-H. Whangbo, A.Bianconi, A.Simon, High temperature superconductivity in sulfur hydride under ultrahigh pressure: A complex superconducting phase beyond conventional BCS, Nov. Supercond. Mater. **2**, 37–42 (2016).
- ¹⁵ S. Ryu and Y. Hatsugai, Topological origin of zero-energy edge states in particle-hole symmetric systems, Phys. Rev. Lett. **89**, 077002 (2002).
- ¹⁶ T.T. Heikkilä and G.E. Volovik, Dimensional crossover in topological matter: Evolution of the multiple Dirac point in the layered system to the flat band on the surface, JETP Lett. **93**, 59 (2011).
- ¹⁷ T.T. Heikkilä, N.B. Kopnin and G.E. Volovik, Flat bands in topological media, JETP Lett. **94**, 233 (2011); arXiv:1012.0905.
- ¹⁸ A.P. Schnyder and S. Ryu, Topological phases and flat surface bands in superconductors without inversion symmetry, Phys. Rev. B **84**, 060504(R) (2011).
- ¹⁹ T.T. Heikkilä and G.E. Volovik, Flat bands as a route to high-temperature superconductivity in graphite, in: *Basic Physics of Functionalized Graphite*, Springer 2016, pp. 123–143, arXiv:1504.05824.
- ²⁰ Hongming Weng, Yunye Liang, Qiunan Xu, Yu Rui, Zhong Fang, Xi Dai, Yoshiyuki Kawazoe, Topological node-line semimetal in three dimensional graphene networks, Phys. Rev. B **92**, 045108 (2015).
- ²¹ Youngkuk Kim, B. J. Wieder, C. L. Kane, A. M. Rappe, Dirac line nodes in inversion symmetric crystals, Phys. Rev. Lett. **115**, 036807 (2015).
- ²² M. Neupane, I. Belopolski, M.M. Hosen, D.S. Sanchez, R. Sankar, M. Szlowska, S.-Y. Xu, K. Dimitri, N. Dhakal, P. Maldonado, P.M. Oppeneer, D. Kaczorowski, F. Chou, M.Z. Hasan, and T. Durakiewicz, Observation of topological nodal fermion semimetal phase in ZrSiS, Phys. Rev. B **93**, 201104 (2016).
- ²³ Y.-H. Chan, C.-K. Chiu, M. Chou, and A. P. Schnyder, Ca₃P₂ and other topological semimetals with line nodes and drumhead surface state, Phys. Rev. B **93**, 205132 (2016),
- ²⁴ G. Bian, T.-R. Chang, R. Sankar, S.-Y. Xu, H. Zheng, T. Neupert, C.-K. Chiu, S.-M. Huang, G. Chang, I. Belopolski, et al., Topological nodal-line fermions in spin-orbit metal PbTaSe₂, Nature communications **7**, 10556 (2016).
- ²⁵ J. Zhao, R. Yu, H. Weng, and Z. Fang, Topological node-line semimetal in compressed black phosphorus, Phys. Rev. B **94**, 195104 (2016).
- ²⁶ M. Hirayama, R. Okugawa, T. Miyake, and S. Murakami, Topological Dirac nodal lines in fcc Calcium, Strontium, and Ytterbium, arXiv:1602.06501.
- ²⁷ H. Huang, J. Liu, D. Vanderbilt, and W. Duan, Topological nodal-line semimetals in alkaline-earth stannides, germanides, and silicides, Phys. Rev. B **93**, 201114 (2016).
- ²⁸ Jianpeng Liu and L. Balents, Correlation and transport phenomena in topological nodal-loop semimetals, arXiv:1609.05529.
- ²⁹ V.V. Dmitriev, A.A. Senin, A.A. Soldatov, A.N. Yudin, Polar phase of superfluid ³He in anisotropic aerogel, Phys. Rev. Lett. **115**, 165304 (2015).
- ³⁰ G.E. Volovik, Superconductivity with lines of gap nodes: Density of states in the vortex, Pisma ZhETF **58**, 457 (1993); JETP Lett. **58**, 469 (1993).
- ³¹ N.B. Kopnin and G.E. Volovik, Singularity of the vortex density of states in *d*-wave superconductors, Pisma ZhETF **64**, 641 (1996); JETP Lett. **64**, 690 (1996).
- ³² G.E. Volovik, Condensation of fermion zero modes in the vortex, Pisma ZhETF **104**, 201 (2016); JETP Lett. **104** (2016).
- ³³ J.W. McClure, Band structure of graphite and de Haas-van Alphen effect, Phys. Rev. **108**, 612-618 (1957).
- ³⁴ D. Pierucci, H. Sediri, M. Hajlaoui, J.-C. Girard, T. Brumme, M. Calandra, E. Velez-Fort, G. Patriarche, M.G. Silly, G. Ferro, V. Souliere, M. Marangolo, F. Sirotti, F. Mauri, and A. Ouerghi, Evidence for flat bands near the Fermi level in epitaxial rhombohedral multilayer graphene, ACS Nano **9**, 5432 (2015).

- ³⁵ L. Tapasztó, G. Dobrik, Ph. Lambin, L.P. Birof, Tailoring the atomic structure of graphene nanoribbons by scanning tunnelling microscope lithography. *Nat Nanotechnol.* **3**, 397 (2008).
- ³⁶ L. P. Birof, P. Lambin, Nanopatterning of graphene with crystallographic orientation control, *Carbon* **48**, 2677 (2010).
- ³⁷ Xinran Wang, Yijian Ouyang, Xiaolin Li, Hailiang Wang, Jing Guo, and Hongjie Dai, Room-temperature all-semiconducting sub-10-nm graphene nanoribbon field-effect transistors, *Phys. Rev. Lett.* **100**, 206803 (2008).
- ³⁸ M. Sprinkle, et al. Scalable templated growth of graphene nanoribbons on SiC. *Nat. Nanotechnol.* **5**, 727–731 (2010)
- ³⁹ Ago, H., Ito, Y., Tsuji, M., Ikeda, K. Step-templated CVD growth of aligned graphene nanoribbons supported by a single-layer graphene film, *Nanoscale* **4**, 5178–5182 (2012).
- ⁴⁰ Hayashi, K., Sato, S., Ikeda, M., Kaneta, C., Yokoyama, N. Selective graphene formation on copper twin crystals, *J. Am. Chem. Soc.* **134**, 12492–12498 (2012).
- ⁴¹ Ago, H. et al. Lattice-oriented catalytic growth of graphene nanoribbons on heteroepitaxial nickel films. *ACS Nano* **7**, 10825–10833 (2013).
- ⁴² R. M. Jacobberger, B. Kiraly, M. Fortin-Deschenes, et al., Direct oriented growth of armchair graphene nanoribbons on germanium, *Nat. Commun.* **6**, 8006 (2015).
- ⁴³ M. Hiramatsu, M. Hori, *Carbon Nanowalls*, Springer-Verlag/Wien, 2010.
- ⁴⁴ X. Shi, Z.-Q. Han, X.-L. Peng, P. Richard, T. Qian, X.-X. Wu, M.-W. Qiu, S.C. Wang, J.P. Hu, Y.-J. Sun, H. Ding, Enhanced superconductivity accompanying a Lifshitz transition in electron-doped FeSe monolayer, arXiv:1606.01470.
- ⁴⁵ P. Esquinazi, T.T. Heikkilä, Yu.V. Lysogorskiy, D.A. Tayurskii, G.E. Volovik, On the superconductivity of graphite interfaces, *Pis'ma ZhETF* **100**, 374 (2014); *JETP Lett.* **100**, 336 (2014).
- ⁴⁶ P. Esquinazi, Graphite and its hidden superconductivity, *Papers in Physics* **5**, 050007 (2013).
- ⁴⁷ A. Ballestar, J. Barzola-Quiquia, T. Scheike, and P. Esquinazi, Josephson-coupled superconducting regions embedded at the interfaces of highly oriented pyrolytic graphite, *New J. Phys.* **15**, 023024 (2013).
- ⁴⁸ A. Ballestar, T.T. Heikkilä, and P. Esquinazi, Interface size dependence of the Josephson critical behaviour in pyrolytic graphite, *Supercond Sci. Technol.* **27**, 115014 (2014)
- ⁴⁹ E. Tang and L. Fu, Strain-induced partially flat band, helical snake states, and interface superconductivity in topological crystalline insulators, *Nature Phys.* **10**, 964 (2014).
- ⁵⁰ A. Gozar, G. Logvenov, L. Fitting Kourkoutis, A. T. Bollinger, L. A. Giannuzzi, D. A. Muller, and I. Bozovic, Interface superconductivity between a metal and a Mott insulator, *Nature* **455**, 782 (2008).
- ⁵¹ Yasushi Kawashima, Possible room temperature superconductivity in conductors obtained by bringing alkanes into contact with a graphite surface, *AIP Advances* **3**, 052132 (2013).
- ⁵² A.N. Ionov, *Pis'ma ZhTF* **41**(13), 79 (2015). *Techn. Phys. Lett.* **41**, 651 (2015)
- ⁵³ A.N. Ionov, Josephson-like behavior of the current-voltage characteristics of multi-graphene flakes embedded in polystyrene, *J. Low Temp. Phys.* **185**, 515 (2016).